

considerations for the novel low-flying TA concept. Section 3 describes the methods developed and used for the preliminary design of the TA. Section 4 presents the results of the design process and compares the DOC of the TA with the DOC of the A320 while Section 5 concludes the paper.

1.2 Reference Aircraft and Reference Mission

The reference aircraft for evaluating the performance of the TA design is the Airbus A320. Key parameters of the A320 are listed in Table 3 in Section 4.3.

The reference mission has a design range of 1510 NM with a payload of 19256 kg. The aircraft is supposed to accommodate 180 passengers in a one-class layout. The cruise Mach number is 0.76. [10]

The proposed TA has the same requirements as the A320 except for a lower cruise Mach number to take account of the speed limitations of TA.

2 Low-Flying Propeller-Driven Aircraft Concept

TA usually have lower cruise speeds than turbofan aircraft. The lower cruise speed results in longer flight times and a possibly reduced number of flights per day. A reduced number of flights leads to a lower productivity of the aircraft and hereby higher seat mile costs which has to be avoided for a competitive aircraft concept. The proposed TA configuration is supposed to have a similar productivity as a turbofan aircraft but, at the same time, a reduced fuel consumption. The high productivity can be reached because of three reasons.

Firstly, the presented turboprop configuration will fly nearly as fast as the reference aircraft A320 which, amongst others, can be realized by reducing the cruise altitude. Fig. 2 shows that a TA flying at a cruise altitude of 6140 m at a feasible turboprop cruise Mach number of 0.71 (the cruise Mach number range of the military transporter Airbus A400M is 0.68 ... 0.72 [4]) would have the same cruise

speed as a turbofan aircraft flying at 11000 m or above with a cruise Mach number of 0.76.

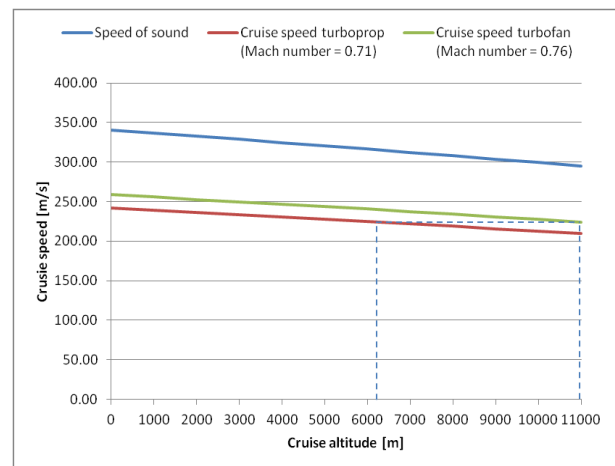


Fig. 2. Reducing the cruise altitude for a given Mach number leads to higher cruise speeds

The cruise altitude reduction of the proposed aircraft concept will be less extreme but still leads to speed improvements as shown in the following example. In Flight Level (FL) 300 (9144 m), a Mach number of 0.71 corresponds to a cruise speed of 215 m/s which is only about 4.4 % lower than the cruising speed of the A320 (which would be 225 m/s for a cruise Mach number of 0.76 in FL 360 (10973 m)).

Secondly, the indicated air speed below FL 100 is limited to 250 knots which means that TA do not lose time during about 20 min of flight shortly after start and before landing under FL 100.

Thirdly, the remaining loss of time is compensated for by a faster turnaround process, for example due to the integration of a continuous cargo compartment into the design as suggested by Kramer [6].

The flight at a lower altitude has consequences for the optimal design of the aircraft. First of all, the aircraft has to be designed for a lower optimal flight level. Secondly, a reduction of the flight altitude results in flights at higher gust speeds and therefore higher gust load factors. Fig. 3 shows that flying at FL 200 leads to an increase of the gust velocity u of about 35 % compared to a flight at FL 360. Equation 1 derived from the lift equation shows that the higher gust velocity together with a speed reduction of 4.4 % (as

shown above) leads to an increase of the load factor change due to gusts Δn of about 29 %. Nevertheless, Δn can be kept at the same level by a 29 % increase of the wing loading of the aircraft.

$$\Delta n = \frac{\rho \cdot u \cdot v \cdot C_{L\alpha}}{2 \cdot \frac{m \cdot g}{S_W}} \quad (1)$$

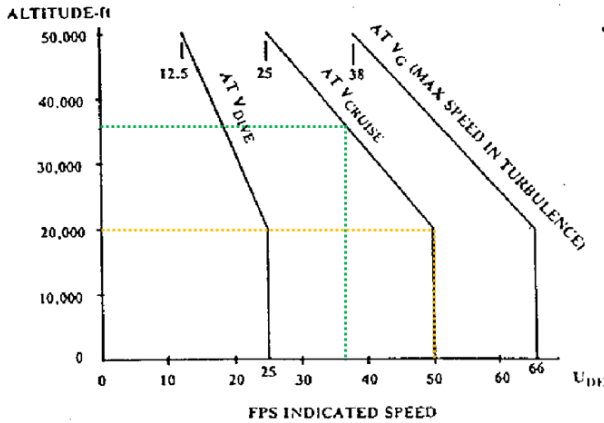


Fig. 3. Derived equivalent gust velocities (from CS-25.341(a)(5), pictured by [17])

The concept of flying lower and faster faces another limit set by an increasing dynamic pressure – in other words a limit defined by an equivalent airspeed V_E as shown in Fig. 4. The structure has also to be designed for loads caused by dynamic pressure. The structure will be heavier if higher equivalent airspeeds are allowed. The concept of the low flying (and light weight) TA would be prepared to find an optimum cruise speed and cruise altitude close to the intersection of the limit defined by maximum operating Mach number and maximum dynamic pressure. This intersection indicates the highest allowable true airspeed and forms a corner in the flight envelope called from now on “speed corner” (SC). The speed corner may offer an interesting high cruise speed, if a high equivalent airspeed is allowed matched by a low cruise altitude. The right black cross in Fig. 4 indicates the usual aircraft position in the flight envelope in the cruise phase. The left black cross shows that the novel low-flying TA could be placed advantageously inside the speed corner. The altitude of the speed corner h_{SC} can be calculated by

$$h_{SC} = \left(1 - \left(\frac{v_E}{M_{MO} \cdot a_0} \right)^{0.3805} \right) \cdot \frac{T_0}{L} \quad (2)$$

where

M_{MO} Maximum operating Mach number

v_E Maximum equivalent airspeed

and

- $a_0 = 340$ m/s
- $T_0 = 288,15$ K
- $L = -0.0065$ K/m

The true airspeed allowed in the speed corner is

$$v = M_{MO} \cdot a_0 \cdot \sqrt{1 - \frac{L \cdot h_{SC}}{T_0}} \quad (3)$$

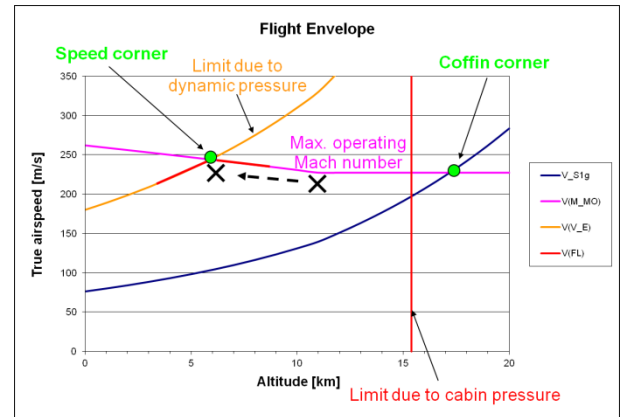


Fig. 4. A very low-flying TA would fly in another area of the flight envelope (adapted from [7])

The high development costs for new aircraft configurations usually are a big challenge. This is another advantage of the proposed novel low-flying TA as it is a conventional configuration with only an unconventional set of design parameters. Techniques and knowledge is already available at Airbus due to the design of the propeller driven Airbus A400M. The engine EPI TP400 developed for the Airbus A400M has a civil certification and a less-powerful derivative of this engine could be used for the proposed aircraft concept which would save additional development costs.

Another challenge for new aircraft configurations like the Blended Wing Body is their integration into the existing aviation system. Existing processes for manufacturing and operation of aircraft have been adapted to

today's conventional tail aft configuration. Unconventional configurations require changes of many processes and therefore incur additional costs. This is one of the primary reasons why many promising unconventional configurations never made it to first flight. In contrast, the proposed configuration can be integrated easily into the existing aviation system.

3 Methods Used and Developed for the Design of the Turboprop Aircraft

For the conceptual design of the proposed TA, the tool ‘‘Turboprop Optimization in Preliminary Aircraft Design’’ (PrOPerA) has been developed. PrOPerA is a further development of the tool ‘‘Optimization in Preliminary Aircraft Design’’ (OPerA) developed by Niță [8]. OPerA has been developed for the preliminary design of turbofan aircraft while PrOPerA can be used for the preliminary design of turboprop driven aircraft. Important methods developed for PrOPerA are described in Section 3.

3.1 Optimum Propeller Design and Propeller Efficiency

The Breguet factor for TA

$$B = \frac{\eta \cdot E}{PSFC \cdot g} \quad (4)$$

emphasizes the importance of a high propeller efficiency for the overall efficiency of a TA. An accurate prediction of the achievable propeller efficiency is therefore crucial for the evaluation of a TA design.

Each TA design can have different requirements concerning cruise speed, flight altitude or thrust. Only propellers designed exactly for these requirements will achieve highest efficiencies. That is why each TA has been designed together with an optimum propeller according to the particular requirements of the aircraft using the method proposed by Adkins and Liebeck [14].

The proposed TA is supposed to fly at high cruise Mach numbers which obviously also lead

to high Mach numbers at the propeller blades decreasing the propeller efficiency and increasing noise [11]. These disadvantages can be reduced by sweeping the propeller blades which decreases the effective Mach number at the blade. Usually the highest Mach number occurs at the tip of the propeller blades. Dubs suggests to limit this Mach number to 0.85 to keep noise in acceptable levels [11]. This requirement for a maximum Mach number at the blade determines the rotational speed of the propeller as shown in the following paragraphs.

According to Torenbeek [12], a sweep angle leads to a reduced effective Mach number of

$$M_{eff} = M \cdot \sqrt{\cos \varphi_{25}} \quad (5)$$

which gives us an equation for the maximum possible Mach number at the blade for a given M_{eff} and φ_{25}

$$M = \frac{M_{eff}}{\sqrt{\cos \varphi_{25}}} \quad (6)$$

Setting M_{eff} to 0.85 and the sweep angle φ_{25} at the propeller tip to 55° (which is the approximate sweep angle at the blade tip of the Ratier-Figeac FH386 propellers used for the military transport aircraft Airbus A400M), leads to a maximum allowed local Mach number M of 1.12 at the blade tip.

At the same time a swept blade has a reduced maximum lift coefficient [17].

$$C_{L,max,swept} = C_{L,max,unswept} \cdot \cos \varphi_{25} \quad (7)$$

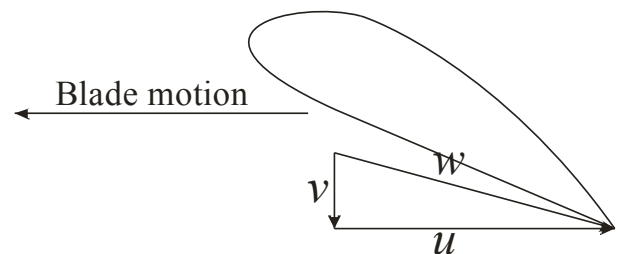


Fig. 5. Airflow at the propeller blade

Fig. 5 shows the local airspeed w at the propeller

$$w = \sqrt{v^2 + u^2} \quad (8)$$

where the circumferential speed u is

$$u = \pi \cdot D \cdot n \quad (9)$$

with the propeller diameter D and the number of rotations per second n .

The freestream velocity v is

$$v = M \cdot a \quad (10)$$

with the speed of sound a .

The calculated maximum Mach number of 1.12 together with D , a and the design cruise speed v_{CR} can be used to determine the rotational speed of the propeller that leads to a maximum effective Mach number at the blade tip of 0.85.

$$n = \frac{\sqrt{(1.12 \cdot a)^2 - v_{CR}^2}}{\pi \cdot D} \quad (11)$$

Setting M_{eff} to 0.85 and M to 1.12 also allows to calculate the sweep angle of all other blade sections using equation 5 and [14].

Swept propeller blades are not considered by the method of Adkins and Liebeck. Therefore the method has been further developed to be able to take account of the effects of sweep. As the method of Adkins and Liebeck also requires profile lift and drag coefficients for various Mach and Reynolds numbers, an airfoil database has been generated by calculating the coefficients using X-foil [13].

The propeller design method finally leads to the optimum chord length, incidence angle and sweep angle at all considered blade sections and the overall propeller efficiency which has been used in the further aircraft design process.

3.2 Landing Gear Design

On the one hand, high propeller diameters reduce the propeller disc loadings which leads to high propeller efficiencies as long as the Mach numbers at the propeller blades do not become too high. On the other hand, high propeller diameters can require high landing gear lengths increasing the mass of the aircraft. To be able to find an optimal trade-off, PrOPerA designs the landing gear for a desired propeller diameter according to the following requirements.

- Tail strike angle $\geq 12.5^\circ$ (Fig. 6) ([17] suggests $10^\circ \dots 15^\circ$)
- Bank angle clearance $\geq 7^\circ$ (Fig. 7) ([16] suggests $6^\circ \dots 8^\circ$)
- Engine ground clearance $\geq 0.25 \cdot D$ (Fig. 7) ([16] suggests $0.25 \cdot$ fan-diameter for turbofan engines)

The requirement for longitudinal tip stability determines the longitudinal position of the main landing gear with respect to the center of gravity of the aircraft

- longitudinal tip stability angle $\geq 15^\circ$ (Fig. 6) [15],

while the requirement for lateral tip stability with a

- lateral tip stability angle $\geq 25^\circ$ [17] (not shown in the figures),

determines the wheel track.

The longitudinal distance between the nose landing gear and the aircraft nose comes from statistics. This distance is based on the space required for the nose landing gear retracting forward into the nose landing gear bay (Fig. 6).

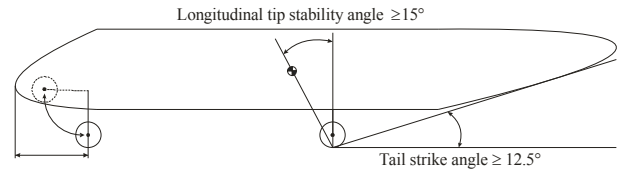


Fig. 6. Requirements for tail-strike, longitudinal tip stability and nose landing gear length

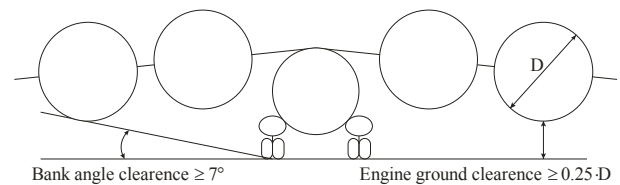


Fig. 7. Bank angle and engine ground clearance requirements. The bank angle clearance has to be checked with respect to every engine and the wing tip

3.3 Engine Parameters

The turboprop engine database of Roux [18] has been used to generate equations for an empirical estimation of important engine parameters as described in sections 3.3.1 and 3.3.2.

3.3.1 Turboprop Engine Mass

Fig. 8 shows the variation of the engine mass m_{eng} with the equivalent take-off power at static sea level $P_{eq,ssl}$ (in kW) for 146 turboprop engines.

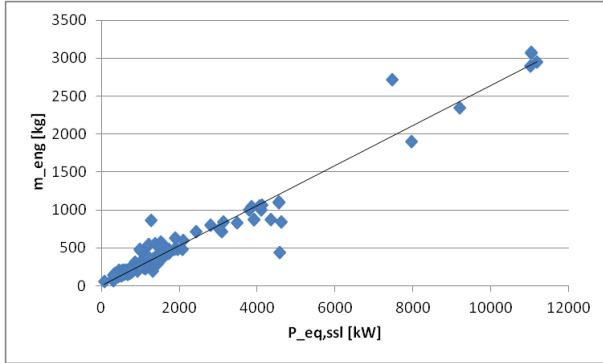


Fig. 8. Engine mass statistic (based on data from [18])

Fig. 8 has been used to obtain a formula for a simple estimation of engine mass

$$m_{eng} = 0.2646 \cdot P_{eq,ssl} \quad (12)$$

with a Pearson product-moment correlation coefficient (PCC) of 0.98. According to [19], this can be evaluated as a direct or indirect linear correlation.

3.3.2 Turboprop Engine Length and Diameter

Fig. 9 shows the variation of the engine length l_{eng} with $P_{eq,ssl}$ (in kW) for 143 turboprop engines.

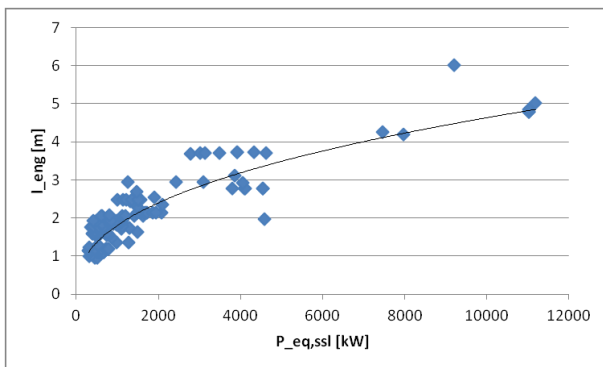


Fig. 9. Engine length statistic (based on data from [18])

Fig. 9 leads to the following formula for a simple estimation of engine length

$$l_{eng} = 0.1068 \cdot (P_{eq,ssl})^{0.4094} \quad (13)$$

with a PCC of 0.87. According to [19], this can be evaluated as a strong correlation.

Fig. 10 shows the variation of the engine diameter d_{eng} with $P_{eq,ssl}$ (in kW) for 143 turboprop engines.

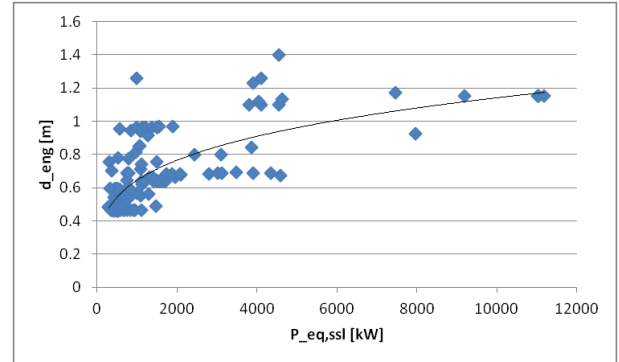


Fig. 10. Engine diameter statistic (based on data from [18])

Fig. 10 leads to the following formula for a simple estimation of engine diameter

$$d_{eng} = 0.1159 \cdot (P_{eq,ssl})^{0.2483} \quad (14)$$

with a PCC of 0.74. According to [19], this can be evaluated as a moderate correlation.

3.4 Power Specific Fuel Consumption

Fig. 11 shows the variation of the Power Specific Fuel Consumption $PSFC$ with the product of $P_{eq,ssl}$ (in kW), the overall pressure ratio $OAPR$ at static sea level and the turbine entry temperature T_{TET} at static sea level (in K) for 88 turboprop engines.

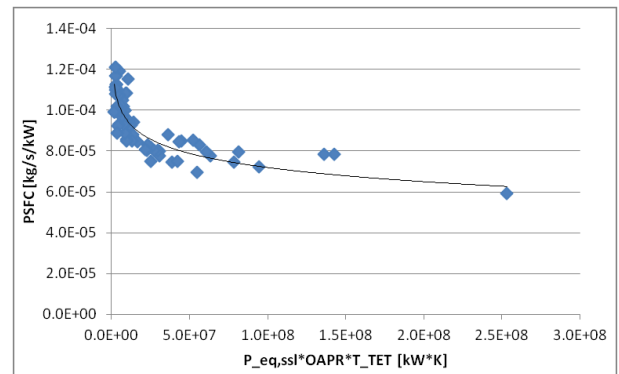


Fig. 11. PSFC statistic (based on data from [18])

Fig. 11 leads to the following formula for a simple estimation of $PSFC$:

$$PSFC = 2,56 \cdot 10^{-4} - \ln(P_{eq,ssl} \cdot OAPR \cdot T_{TET}) \cdot 10^{-5} \quad (15)$$

with a PCC of 0.86. According to [19], this can be evaluated as a strong correlation.

3.5 Landing Field Length and Maximum Lift Coefficient at Landing

According to Scholz [21], the approach speed v_{APP} can be calculated from the landing field length s_{LFL} with

$$v_{APP} = k_{APP} \cdot \sqrt{s_{LFL}} \quad (16)$$

For turboprop driven aircraft

$$k_{APP} = 1.70 \sqrt{m/s^2} \quad (17)$$

is suggested. Fig. 12 presents the variation of s_{LFL} with the square of v_{APP} for 15 turboprop driven aircraft with an initial service date between 1988 ... 1999.

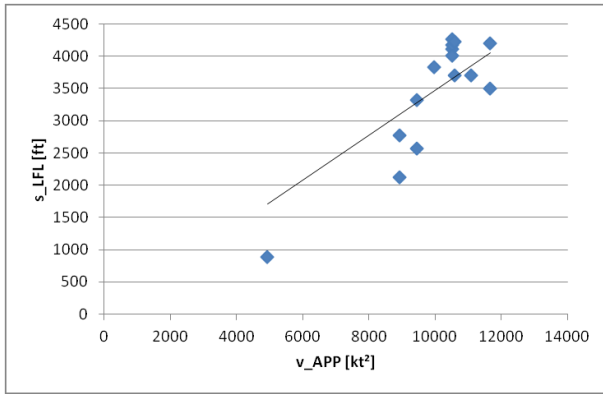


Fig. 12. FAR landing field length of turboprop driven aircraft

The figure leads to

$$k_{APP} = 1.58 \sqrt{m/s^2} \quad (18)$$

The PCC is 0.83 which is a strong correlation according to [19]. The result shows that present turboprop driven aircraft show inferior breaking performance compared to turboprop driven aircraft. Newly designed aircraft may show better breaking performance with state of the art anti skid breaking systems with a k_{APP} even larger than $1.7 (m/s^2)^{0.5}$. The possibility of turboprop driven aircraft having even a shorter landing field length than turboprop aircraft for the same wing loading is enabled by a lower safety factor in the definition of the landing field length of turboprops ($1/0.7 = 1.43$) compared to that for turboprops ($1/0.6 = 1.67$) [25]. For the design of the TA, $k_{APP} = 1.70 (m/s^2)^{0.5}$ has been assumed.

The maximum lift coefficient at landing $C_{L,max,L}$ of those aircraft has also been analyzed to get an average value for preliminary aircraft design (shown in Fig. 13).

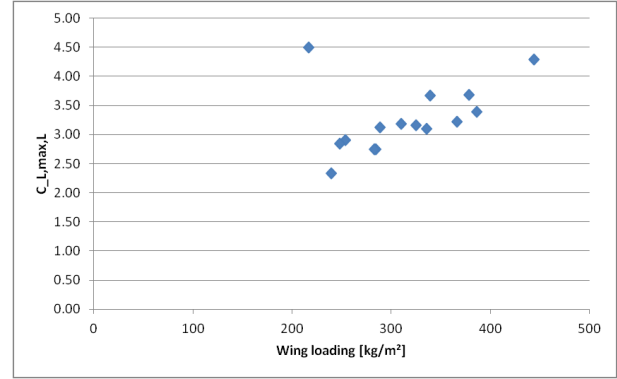


Fig. 13. Maximum lift coefficient at landing of turboprop driven aircraft

The figure leads to an average value of

$$C_{L,max,L} = 3.25. \quad (19)$$

Such k_{APP} and $C_{L,max,L}$ analysis has also been performed for older TA. The results of that analysis are shown in Table 1. Breaking performance (expressed through k_{APP}) and lift coefficient at landing $C_{L,max,L}$ have improved slowly over the decades.

Table 1. Results of a statistical analysis of k_{APP} and $C_{L,max,L}$ for turboprop driven aircraft

Initial service date	k_{APP} [$(m/s^2)^{0.5}$]	$C_{L,max,L}$
1958 ... 1973	1.53	3.12
1974 ... 1987	1.54	3.00
1988 ... 1999	1.58	3.25

3.6 Take-off Field Length and Maximum Lift Coefficient at Take-off

According to Scholz [21], the take-off field length s_{TOFL} can be calculated using the following equation:

$$s_{TOFL} = k_{TO} \cdot \frac{m_{MTO}^2 \cdot g}{S_W \cdot T_{TO} \cdot \sigma \cdot C_{L,max,TO}} \quad (20)$$

For turbofan driven aircraft

$$k_{TO} = 2.34 \frac{m^3}{kg} \quad (21)$$

is suggested.

Fig. 14 presents the variation of s_{TOFL} with

$$\frac{m_{MTO}^2 \cdot g}{S_W \cdot T_{TO} \cdot \sigma \cdot C_{L,max,TO}} \quad (22)$$

for 17 turboprop driven aircraft with an initial service date between 1974 ... 1995. A longer time period compared to the calculation of k_{APP} was chosen because the previously used shorter time period did not lead to statistically significant results.

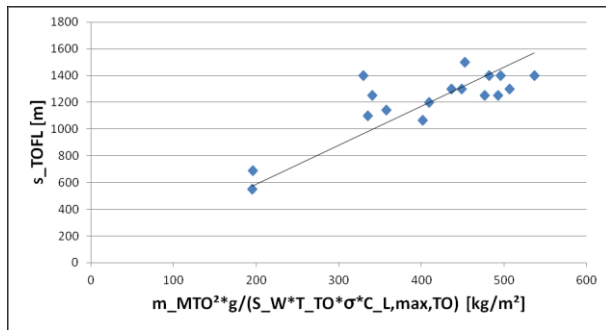


Fig. 14. FAR take-off field length of turboprop driven aircraft

The figure leads to

$$k_{TO} = 2.92 \frac{m^3}{kg} \quad (23)$$

The PCC is 0.74 which is a moderate correlation according to [19].

The maximum lift coefficient at take-off $C_{L,max,TO}$ of 8 aircraft with an initial service date between 1988 ... 1995 has also been analyzed to get an average value for preliminary aircraft design (shown in Fig. 15).

The figure leads to an average value of

$$C_{L,max,TO} = 2.27. \quad (24)$$

Such k_{TO} and $C_{L,max,TO}$ analysis has also been performed for older TA. The results of that analysis are shown in Table 2. Surprisingly the take-off performance (expressed through k_{TO}) has deteriorated over the decades while the average take-off lift coefficient $C_{L,max,TO}$ of the

latest time period is about 24 % higher than that of the first considered time period.

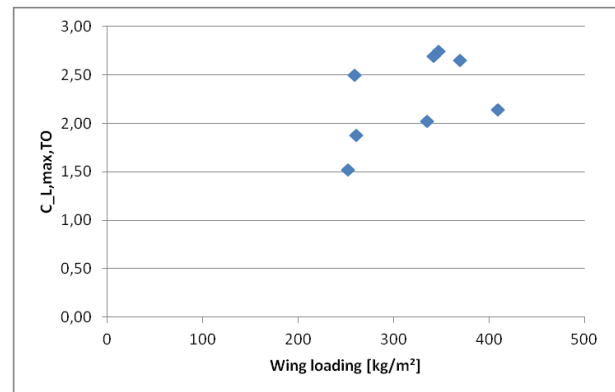


Fig. 15. Maximum lift coefficient at take-off of turboprop driven aircraft

Table 2. Results of a statistical analysis of k_{TO} and $C_{L,max,TO}$ for turboprop driven aircraft

Initial service date	k_{TO} [m ³ /kg]	$C_{L,max,TO}$
1958 ... 1973	2.46	1.83
1974 ... 1987	2.92	2.34
1988 ... 1995		2.27

4 Aircraft Design Results

In this section the results of the TA design with PrOPerA are presented. First of all an overall aircraft configuration had to be chosen which is described in Section 4.1. After that a manual parameter variation (described in Section 4.2) has been performed aimed at finding optimum aircraft parameters for minimum DOC. The final TA design is presented in Section 4.3.

4.1 Choosing the Turboprop Aircraft Configuration

Fig. 16 shows the variation of the ratio between the DOC of the TA and the DOC of the A320 with the propeller diameter. The red line marks a ratio of 1 which means that the DOC of the TA and the A320 are equal at that line. Aircraft designs lying below the red line indicate that the DOC of the TA are lower than the DOC of the A320 and vice versa. For all DOC calculations presented in this paper, the DOC method

proposed by the Association of European Airlines has been used [20].

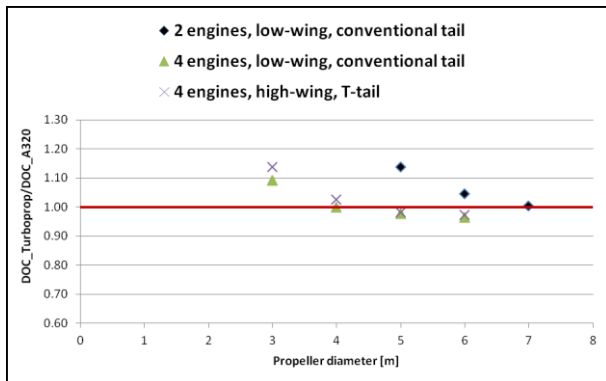


Fig. 16. DOC comparison between TA and the A320 for different propeller diameters

The blue dots in Fig. 16 show the DOC ratio of a TA having two engines, a low wing and a conventional tail. All other requirements are the same as those for the A320 (described in Section 1.2). It can be seen that the DOC of such a TA are worse than the DOC of the A320. This is mainly because of two reasons. Firstly such TA have high thrust-to-weight ratio requirements coming, amongst others, from the mandatory minimum climb gradient in the 2nd segment with one engine inoperative. This leads to high design thrust-to-weight ratios always impairing the overall efficiency of an aircraft. Secondly those TA have to be operated at high disc loadings leading to low propeller efficiencies and therefore also impairing the overall aircraft efficiency.

One option to reduce the requirement coming from the 2nd segment is the use of 4 engines. The green triangles in Fig. 16 show the results for TA having 4 engines without changing the rest of the configuration or any other requirement. It can be seen that this leads to high improvements of the DOC. Because of the lower thrust-to-weight requirement from the 2nd segment, the overall thrust-to-weight ratio is lower with positive effects on the overall aircraft efficiency overcompensating the higher maintenance costs of 4 engines.

As mentioned in Section 2, the TA is supposed to have a continuous cargo compartment which can be achieved by a high wing configuration. The purple crosses in Fig. 16 show the results of the design of such a

high wing TA having 4 engines and a T-tail to lift the horizontal tail out of the wake of the inner turboprops. Again all other requirements stay the same. It can be seen that the DOC of high and low wing TA designs are similar. On the one hand a high wing aircraft has the advantage of a shorter and therefore lighter landing gear than a low wing aircraft. But on the other hand, the T-tail of the high wing aircraft is heavier than the conventional tail of the low wing aircraft. Additionally the landing gear compartments lying outside the fuselage increase the wetted area of the aircraft and cause additional drag.

In general, it can be seen that the higher the propeller diameter, the lower the DOC. This effect declines at high propeller diameters because of high required landing gear lengths increasing the operating empty mass of the aircraft.

For the presented TA designs, the propeller diameters have been limited by the requirement that the outer engine position has to be within a certain ratio of the halfspan of the wing. Engines positioned too close to the tip of the wing might cause flutter-problems. Because flutter has not been investigated within the scope of this paper, a conservative maximum propeller diameter of 6 m has been chosen. This diameter leads to a maximum ratio of 0.77 between the outer engine position and the halfspan of the wing. The distance between two propellers has been set to 0.26 m while the distance between propeller and fuselage has been set to 1.01 m. Both distances come from own statistics.

Based on the described design results, it was decided to continue the TA design with a high wing configuration having 4 engines, a propeller diameter of 6 m and a T-tail.

4.2 Parameter Variation and Influence of Cruise Altitude

4.2.1 Manual Parameter Variation

After choosing the aircraft configuration, the influence of Mach number on the DOC has been investigated. The yellow squares in Fig. 17 show the variation of the DOC ratio with the

cruise Mach number. It can be seen that Mach numbers in the range of 0.71 provide the lowest DOC for the TA. Below that range, the number of flights per year becomes too low even though the propeller efficiency increases slightly. Above that range, the considerable decrease of the propeller efficiency predominates the higher number of flights per year. Based on these results, a Mach number of 0.71 has been chosen.

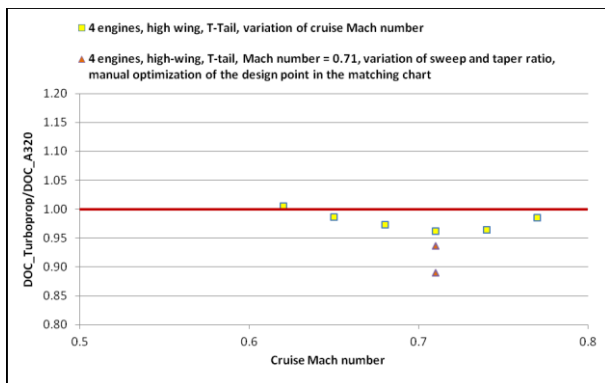


Fig. 17. DOC comparison between TA and the A320 for different cruise Mach numbers and further parameter variations

In a next step more aircraft parameters have been varied manually to further decrease the DOC ratio. Amongst others, the wing sweep has been changed from 25° to 15° due to the lower cruise Mach number of the TA. The taper ratio has been changed from 0.213 (for the A320) to 0.2 which should be the minimum for the taper ratio according to [21]. A further manual adaption of the TA design point aimed at low thrust-to-weight ratios and high wing loadings finally leads to a trip fuel mass reduction of about 13.9 % (on a stage length of 755 NM which has also been used for DOC calculations) and a 6.3 % DOC reduction (the upper purple triangle in Fig. 17) while the landing field length can be reduced by 6.1 %. The manual parameter variation indicated further DOC reduction potential by changing the ratio between the maximum lift coefficients at take-off and landing. This will be investigated in upcoming project stages.

In a final step, two aircraft parameters have been estimated less conservatively. Firstly the additional required soundproofing material due to the use of turboprop engines had to be estimated roughly due to the complexity of

noise considerations. For all previously presented aircraft designs, [22] led to an estimation of 1000 kg of additional required soundproofing material mass. Considering the technical progress between [22] and today, a less conservative estimation of 500 kg also seems to be reasonable.

Secondly, the maintenance costs per turboprop engine have been estimated conservatively using [22]. This report says that the maintenance costs of a turboprop engine are 1.74 times higher than the costs of a comparable turbofan engine. But, based on a recent expert interview [23], nowadays turboprop maintenance costs are even lower than the costs of comparable turbofan engines. According to [23], this is because of lower turbine entry temperatures and lower engine complexity. As a compromise, it is assumed that the maintenance costs of comparable turbofan and turboprop engines are equal.

The lower purple triangle in Fig. 17 shows the DOC of a TA using these two less conservative assumptions for soundproofing material mass and turboprop engine maintenance costs. Such a TA design leads to a trip fuel mass reduction of about 14.9 % (again on a stage length of 755 NM which has also been used for DOC calculations) and a DOC improvement of about 11 % while the landing field length can be reduced by 6.1 %.

A simplified analysis of the DOC of the A320neo using OPerA showed that the DOC of the A320neo are 3.9 % lower than the DOC of the A320. Comparing the DOC of the previously described TA to the DOC of the A320neo therefore still leads to a potential DOC reduction of about 7.3 %.

4.2.2 Influence of Cruise Altitude

The design results confirm that the Cruise Altitude (CA) of the chosen TA configuration is lower (13.4 %) than the CA of the A320. Nevertheless the change in CA is lower than expected. This is because the CA of the aircraft is mainly driven by the chosen design point in the matching chart where the design wing-loading (WL) determines the CA. A lower design WL leads to a lower CA and vice versa. For example, the design WL in Fig. 18 is

640 kg/m² which leads to a CA of 11335 m while the design WL of the chosen TA configuration in Fig. 19 is 601 kg/m² leading to a CA of 10266 m. As the design point in Fig. 19 leads to lower DOC, it is, in this case, better to fly at a lower WL and therefore a lower CA. A further reduction of the WL and therefore the CA would impair the DOC again as shown in Fig. 20. At such a WL, the positive effect of higher cruise speeds at lower CAs (as explained in Section 2) is overcompensated by the negative effect of a badly chosen design point in the matching chart. In Fig. 20, it can be seen that there is a CA providing minimum DOC. This is the CA that comes from the optimum WL in the matching chart.

In summary the proposed TA concept flies at lower altitudes but due to a different reason than initially expected.

Now that the aircraft has been sized, the equivalent airspeed and hence the dynamic pressure can be lowered according to the resulting design cruise altitude h_{CR} (Fig. 21). This helps to save structural weight. The maximum allowed equivalent airspeed for the design could be set to

$$v_E = M_{MO} a_0 \left(1 - \frac{L \cdot h_{CR}}{T_0} \right)^{2.628} \quad (25)$$

This would now place the speed corner according to the design cruise altitude optimizing aircraft weight. Care should be taken that

- $v_E > 250$ kt

because the permissible maximum speed below FL 100 set by ATC should be reached for not increasing flight time and

- $v_E > M_{MO} a_0 \left(1 - \frac{L h_T}{T_0} \right)^{2.628}$

where

h_T Altitude of the tropopause (11 km)

for not limiting the operating Mach number in the stratosphere even if the design cruise altitude is higher for not increasing flight time if for operational reasons cruise altitude is limited on a particular day.

Changes in aircraft structural mass with changes in v_E and hence dynamic pressure have

not been taken into account in this study. Further research will also look at the saving potential of defining an optimum speed corner.

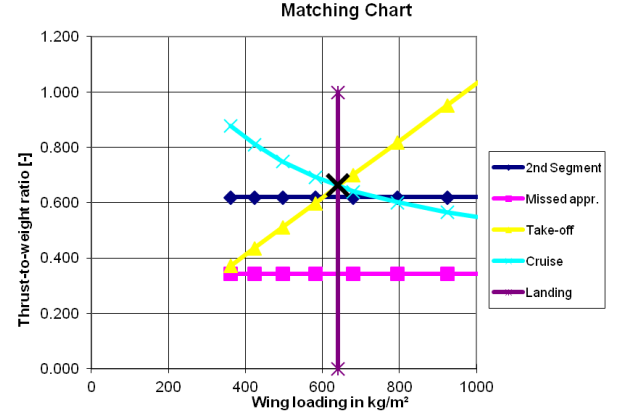


Fig. 18. Matching chart leading to a higher cruise altitude

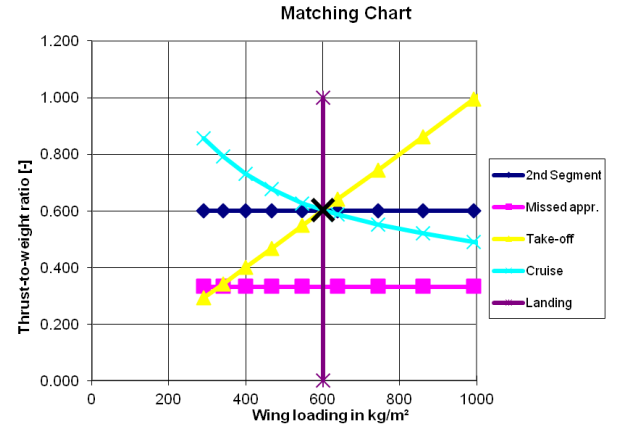


Fig. 19. Matching chart of the manually optimized TA flying at a lower cruise altitude

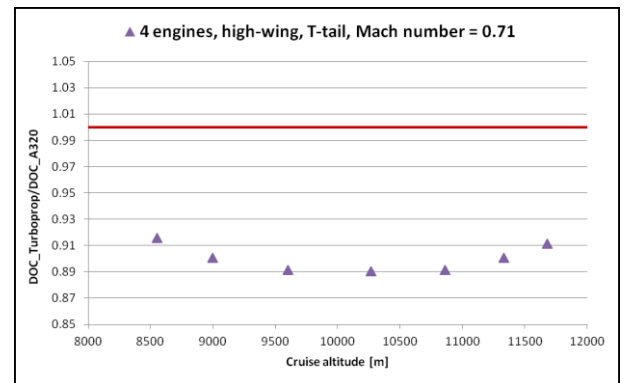


Fig. 20. Variation of the DOC with cruise altitude

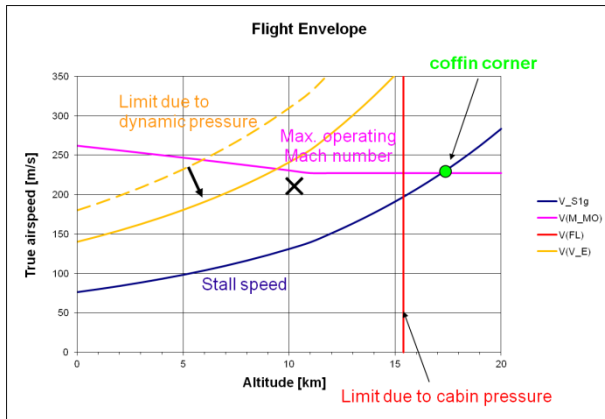


Fig. 21. Lowering the maximum equivalent airspeed of the proposed TA and matching the speed corner to the design could offer structural weight savings (adapted from [7])

4.3 Description of the Favored Turboprop Aircraft Design

Table 3 shows key parameters for a comparison between the proposed TA and the reference aircraft A320. The values for the A320 are taken from a redesign of Niță [8] using OPerA.

It can be seen that the values for $C_{L,max,L}$ and $C_{L,max,TO}$ of the TA are 6.6 % higher than those of the A320. This is due to the lower sweep angle of the TA and due to the assumption that the coefficients of TA and A320 would be equal for an unswept wing. The glide ratio E of the TA and the A320 has been estimated using the method of Niță and Scholz [24] for the calculation of the Oswald efficiency factor.

Table 3. Comparison of key parameters of the proposed TA and the A320

Parameter	TA	A320	Deviation [%]
m_{OE} [kg]	31785	41244	-22.9
m_{MZF} [kg]	51041	60500	-15.6
m_{MTO} [kg]	62069	73500	-15.6
$m_{F,trip}$ [kg]	4817	5663	-14.9
S_W [m ²]	103.2	122.4	-15.8
S_{LFL} [m]	1360	1448	-6.1
h_{CR} [m]	10266	11861	-13.4
v_{CR} [m/s]	212	224	-5.4
E [-]	17.76	17.59	+1.0
$C_{L,max,L}$ [-]	3.28	3.07	+6.6
$C_{L,max,TO}$ [-]	2.85	2.68	+6.6

where

- m_{OE} Operating empty mass
- m_{MZF} Maximum zero-fuel mass
- m_{MTO} Maximum take-off mass
- $m_{F,trip}$ Trip fuel mass (stage length = 755 NM)
- S_W Wing area
- S_{LFL} Landing field length

Table 4 shows more key parameters of the proposed TA.

Table 4. Additional key parameters of the proposed TA

Parameter	Value
$P_{eq,ssl}$ [kW]	6924
η [%]	84.4
$PSFC$ [kg/W/s]	$6.36 \cdot 10^{-8}$
DOC [%]	-11

$P_{eq,ssl}$ has been calculated using the method proposed by Howe [26] which has been corrected with the help of statistics.

Fig. 22 shows a mass breakdown of the proposed TA and the A320. For instance the vertical tail mass of the TA is 2.3 % of its m_{OE} while the vertical tail mass of the A320 is only 1.7 % of its m_{OE} . This is caused by the T-tail configuration of the TA where the vertical tail also has to carry the weight and loads of the horizontal tail.

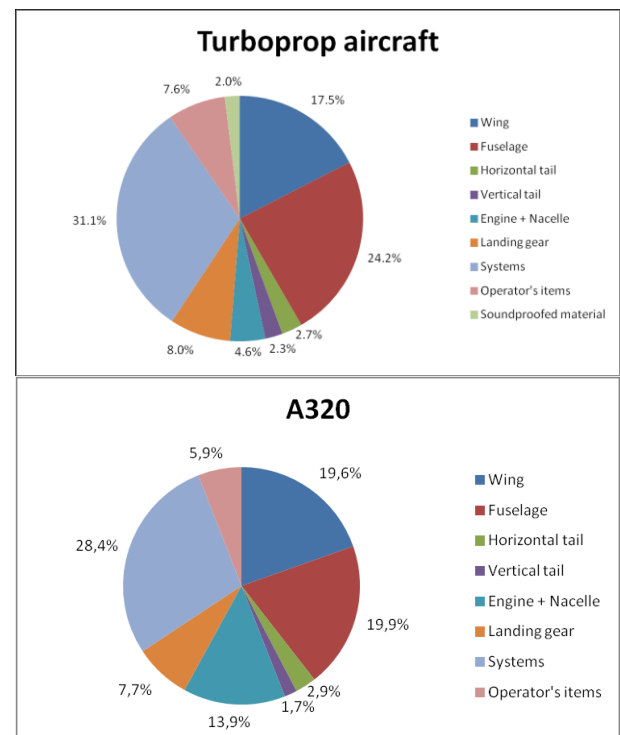


Fig. 22. Mass breakdown of the TA and the A320

Additionally the aircraft has been modeled using “Plane Maker” which is a part of the flight simulator “X-Plane” [9]. The aircraft model has been used successfully for flight simulations and is shown in Fig. 23 and Fig. 24.

Striking features are

- the big propellers with a diameter of 6 m because of high propeller efficiencies at high propeller diameters due to low disc loadings
- the swept propeller blades keeping the Mach number at the entire blade ≤ 0.85
- the big main landing gear compartments at the outside of the fuselage because of the high wing configuration and the requirement for a continuous cargo compartment
- the T-tail lifting the horizontal tail out of the propeller wake

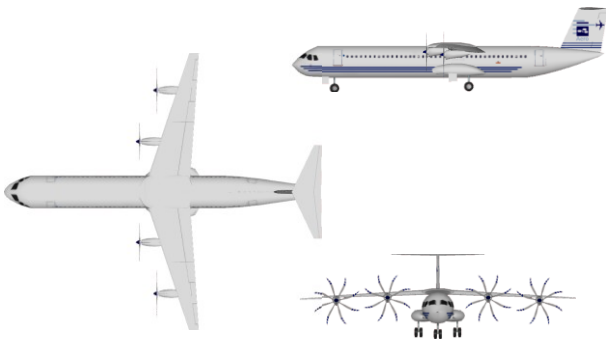


Fig. 23. Three view of the SmartTurboprop



Fig. 24. SmartTurboprop

Being able to derive an aircraft family is one important requirement for every new aircraft concept. Fig. 25 therefore shows a stretched and a shortened version of the proposed TA. The pictured stretched version is able to carry the same passenger (PAX) number as the Airbus A321 while the shortened version

is able to carry the same PAX number as the A319.

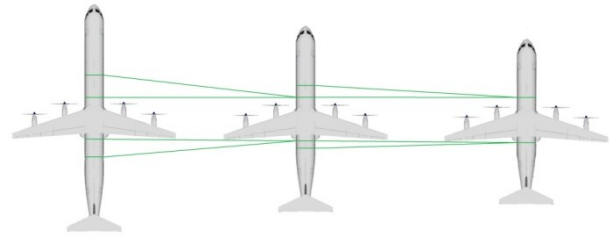


Fig. 25. Family concept for the proposed TA

The ground handling of the aircraft is another important aspect for evaluating the feasibility of a new aircraft concept. Fig. 26 shows the ground handling at the gate of the standard version of the proposed TA. Fig. 27 shows the ground handling at the gate of the shortened version usually causing most problems concerning ground handling within an aircraft family. For the standard version, only minor changes of the ground handling process are required compared to the ground handling of the A320 described in [10]. The right outer turboprop engine blocks the space where the fuel tanker (FUEL) and one Unit Load Device (ULD) train are positioned during the A320 turnaround. This problem can be solved easily by moving the fuel tanker to the right end of the wing and the ULD train to the lower right area.

The ground handling process of the shortened version stays the same except that there is no more space for the conveyor belt vehicle (CB) at the rear part of the fuselage. The lower deck cargo loader (LD CL) and the CB therefore have to share one door and have to be used one after the other.

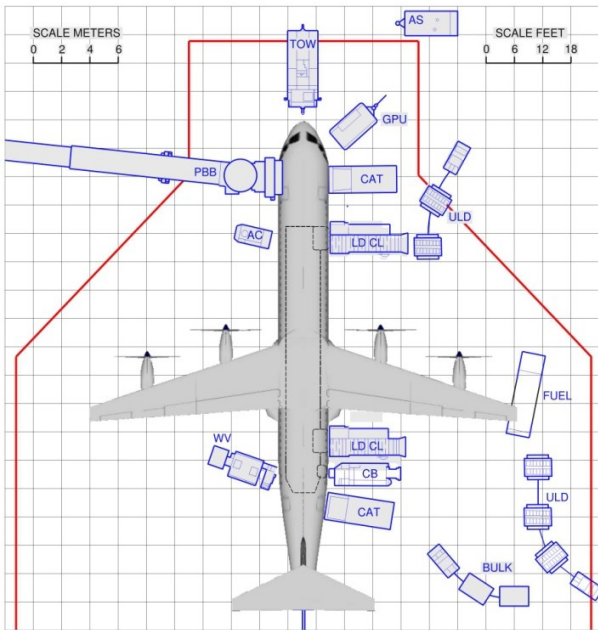


Fig. 26. Ground handling at the gate of the standard version (adapted from [10])

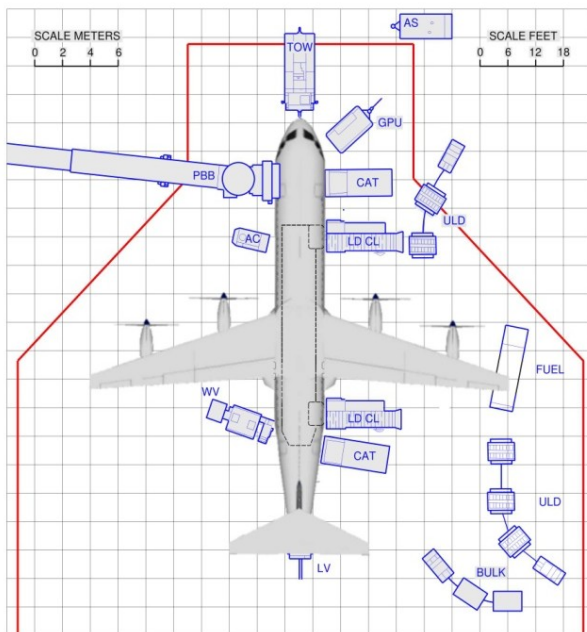


Fig. 27. Ground handling at the gate of a shorter version (adapted from [10])

5 Summary and Conclusion

The proposed turboprop driven aircraft concept has the potential of reducing DOC by about 11 % while reducing fuel consumption and therefore CO₂ emissions by about 14.9 % at a DOC range of 755 NM. The DOC reduction mainly comes from the lower specific fuel

consumption of turboprop engines compared to turbofan engines causing additional positive snowball effects. The potential savings are mainly decreased by additional weight due to the T-tail configuration, higher landing gear lengths caused by high propeller diameters and additional required soundproofing material due to the propeller noise. As the calculated DOC reduction is probably not high enough to justify the development of a new aircraft family, the proposed TA concept has to be further improved to be able to become a potential successor of the A320-family. Therefore the potential of the future technologies

- laminar flow
- braced wing
- distributed propulsion

in combination with the proposed TA concept will be further investigated in upcoming stages of the research project.

Acknowledgements

The authors acknowledge the financial support of the German Federal Ministry of Education and Research (BMBF) which made this work possible. The authors would like to thank Axel Dengler and colleagues from Airbus for interesting discussions and the exchange of ideas.

References

- [1] European Commission. *Flightpath 2050 Europe's Vision for Aviation*. Aerodays, Madrid, 2011. – URL: <http://ec.europa.eu/transport/air/doc/flightpath2050.pdf> (2012-07-09)
- [2] URL: http://www.airport2030.de/Airport2030_de.html, July 9, 2012.
- [3] Babikian R, Lukacho S.P. and Waitz, I.A. The historical fuel efficiency characteristics of regional aircraft from technological, operational, and cost perspectives. *Journal of Air Transport Management*, Vol. 8, No. 6, pp 389-400, 2002. – URL: http://web.mit.edu/aeroastro/people/waitz/publication_s/Babikian.pdf (2012-07-09)
- [4] URL: <http://www.airbusmilitary.com/Aircraft/A400M/A400MSpec.aspx>, July 9, 2012.

- [5] Jackson P. *Jane's All the World's Aircraft 2008-2009*. Jane's information Group, Coulsdon, Surrey, United Kingdom, 2008.
- [6] Krammer P, Junker O and Scholz D. *Aircraft design for low cost ground handling – The final results of the Aloha project*. 27th International Congress of the Aeronautical Sciences, Nice, France, 2010. – URL: <http://ALOHA.ProfScholz.de> (2012-07-09)
- [7] Scholz D. *Flugbereichsgrenzen - Flight Envelope*. Appendix to the flight mechanics lecture notes, Hamburg University of Applied Sciences, Hamburg, Germany, 2012. – URL: <http://FM1.ProfScholz.de> (2012-07-09)
- [8] Niță M. *Contributions to Aircraft Preliminary Design and Optimization*. Doctoral Thesis, Politehnica University of Bucharest, Faculty of Aerospace Engineering, 2012.
- [9] URL: <http://www.x-plane.com>, July 9, 2012.
- [10] AIRBUS S.A.S. *A320 AIRPLANE CHARACTERISTICS FOR AIRPORT PLANNING*. Issue: Sep 30/85, Rev: May 2011. – URL: http://www.airbus.com/fileadmin/media_gallery/files/tech_data/AC/Airbus-AC-A320-Jun2012.pdf (2012-07-09)
- [11] Dubs F. *Aerodynamik der reinen Unterschallströmung*, 4th edition, 1979.
- [12] Torenbeek E. *Synthesis of subsonic airplane design*. Delft University Press, Delft, 1988.
- [13] URL: <http://web.mit.edu/drela/Public/web/xfoil/>, July 9, 2012.
- [14] Adkins C and Liebeck R. Design of optimum propellers. *Journal of Propulsion and Power*, Vol. 10, No. 5, pp 676-682, 1994.
- [15] Currey N S. *Aircraft landing gear design: Principles and practices*. AIAA Education Series, Washington D.C., AIAA, 1988.
- [16] Trahmer B. *Fahrwerk - Fahrwerksintegration in den Gesamtentwurf*. Aircraft design lecture, Hamburg University of Applied Sciences, Hamburg, Germany, 2004. – URL: <http://FE.ProfScholz.de> (2012-07-09)
- [17] Raymer D P. *Aircraft Design : A Conceptual Approach*. AIAA Education Series, Washington D.C., AIAA, 1989.
- [18] Roux É. *Turboshaft, Turboprop & Turbofan Database Handbook*, Éditions Élodie Roux, 2011.
- [19] Arbeitskreis Masseanalyse. *Luftfahrttechnisches Handbuch, Band Masseanalyse*. Industrieanlagen-Betriebsgesellschaft (IABG), 2008.
- [20] Association of European Airlines. *Short-Medium Range Aircraft AEA Requirements*. Brussels, AEA, 1989. (G(T)5656)
- [21] Scholz D. *Skript zur Vorlesung Flugzeugentwurf*. Hamburg, Fachhochschule Hamburg, FB Fahrzeugtechnik, Abt. Flugzeugbau, Vorlesungsskript, 1999. – URL: <http://FE.ProfScholz.de>
- [22] Schulz H G and Fischer B. *Integration von Propfans im Flugzeugentwurf*. MBB, Ziviles Komponenten Programm, Schlußbericht, UT-013/86, 1986.
- [23] Bräunling W. Expert interview by telephone. June 29, 2012.
- [24] Niță M and Scholz D. *Estimating the Oswald Factor from Basic Aircraft Geometrical Parameters*. 61. Deutscher Luft- und Raumfahrtkongress 2012, Berlin, Germany, 2012.
- [25] European Aviation Safety Agency. *Certification Specifications for Large Aeroplanes CS-25*, 2003.
- [26] Howe D. *Aircraft Conceptual Design Synthesis*. London, Professional Engineering Publishing, 2000.

Copyright Statement

The authors confirm that they, and/or their company or organization, hold copyright on all of the original material included in this paper. The authors also confirm that they have obtained permission, from the copyright holder of any third party material included in this paper, to publish it as part of their paper. The authors confirm that they give permission, or have obtained permission from the copyright holder of this paper, for the publication and distribution of this paper as part of the ICAS2012 proceedings or as individual off-prints from the proceedings.